inorganics

MDPI

Review

A Comprehensive Study on the Applications of Clays into Advanced Technologies, with a Particular Attention on Biomedicine and Environmental Remediation

Roberto Nisticò

Department of Materials Science, University of Milano-Bicocca, Via R. Cozzi 55, 20125 Milano, Italy; roberto.nistico@unimib.it; Tel.: +39-02-6448-5111

Abstract: In recent years, a great interest has arisen around the integration of naturally occurring clays into a plethora of advanced technological applications, quite far from the typical fabrication of traditional ceramics. This "second (technological) life" of clays into fields of emerging interest is mainly due to clays' peculiar properties, in particular their ability to exchange (capture) ions, their layered structure, surface area and reactivity, and their biocompatibility. Since the maximization of clay performances/exploitations passes through the comprehension of the mechanisms involved, this review aims at providing a useful text that analyzes the main goals reached by clays in different fields coupled with the analysis of the structure-property correlations. After providing an introduction mainly focused on the economic analysis of clays global trading, clays are classified basing on their structural/chemical composition. The main relevant physicochemical properties are discussed (particular attention has been dedicated to the influence of interlayer composition on clay properties). Lastly, a deep analysis of the main relevant nonconventional applications of clays is presented. Several case studies describing the use of clays in biomedicine, environmental remediation, membrane technology, additive manufacturing, and sol-gel processes are presented, and results critically discussed.

Keywords: alumino-silicates; biomedicine; ceramics; clays; inorganic chemistry; environmental remediation; nanomaterials; porous materials

Citation: Nisticò, R. A Comprehensive Study on the Applications of Clays into Advanced Technologies, with a Particular Attention on Biomedicine and Environmental Remediation. *Inorganics* **2022**, *10*, 40. https://doi.org/10.3390/inorganics10030040

Academic Editor: Carlos Martínez-Boubeta

Received: 18 February 2022
Accepted: 19 March 2022
Published: 21 March 2022

1. Introduction

Clays are naturally occurring 2D layered fine particles (less than 2 μm) extracted from earth and composed of phyllosilicates (clay minerals), showing plastic properties at appropriate water content and brittleness upon drying or firing (i.e., hardening processes) [1,2]. These very peculiar properties are strictly related to clays' chemical structure, and in particular to specific chemical reactions occurring at the surface/interface of these layered materials [3,4]. Such interfacial phenomena are the basis of the recent grown interest around clays (i.e., one of oldest class of materials handled and modeled by humans) as alternative (nanoscopic) materials. Scientific and engineering field of emerging interest where clays can be exploited such as biomedicine [5–9], environmental clean-up processes [10–18], membrane technologies [19–22], energetic and electronic applications [23–26], composite materials [27–33], sol-gel technology [34,35], 3D printing [36,37], and in developing traditional ceramics (i.e., earthenware, stoneware, porcelain, pottery, and so on) [38–40] are numerous.

The recent attention around the exploitation of 2D layered materials (e.g., graphene [41], and its derived graphene oxide (GO), carbon nitride (g-C_3N_4), molybdenum disulfide (MoS_2) [42], tungsten diselenide (WSe_2), tin sulfide (SnS_2), tin diselenide ($SnSe_2$), boron nitride (BN), and black phosphorous (P allotrope)) has also raised the interest concerning the exploitation of clays as naturally occurring layered materials. Furthermore, as pointed out in the literature [2,43,44], clays are largely diffused (almost worldwide in nature) in

consistent amounts. The exploitation of clays guarantees a twofold advantage in terms of economic sustainability (i.e., low cost of raw materials) and environmental safety, coupled with their availability also in developing countries [45,46]. Therefore, the valorization of clays follows the principles at the basis of the circular economy [47–49], and analogously as in the cases of biomasses [50–54], biochars [55–59], and biofuels [60,61], clays can play a major role in the green chemistry-driven technological revolution.

From the economic viewpoint, actually clays represent raw materials of remarkable interest for the global market (i.e., clays accounted for 0.012% of total world trade in 2019). Countries leading in the extraction/exportation of clays are the US (USD 389 million, covering almost 18.2% of the global market), China (USD 260 million, 12.1%), Ukraine (USD 197 million, 9.2%), Germany (USD 166 million, 7.8%), India (USD 105 million, 4.9%), Turkey (USD 101 million, 4.7%), Spain (USD 93 million, 4.4%), and France (USD 84 million, 3.9%) [62]. Italy is the 7th largest European exporter with approximately USD 48 million (corresponding to approximately 2.2% of the global market). Interestingly, Italy is the largest global importer with a value of approximately 8.9% of the global market (ca. USD 191 million), followed by Germany (USD 180 million, 8.4%), the Netherlands (USD 142 million, 6.6%), Poland (USD 104 million, 4.9%), Japan (USD 95 million, 4.4%), and Canada (USD 93 million, 4.4%) [63]. Moreover, the growth of the previously cited nonconventional advanced applications is going to significantly increase the global trading of clays within the next few years.

The aim of this document is to provide a critical analysis of the potential nonconventional uses of clays into technological fields of emerging interest. Particular emphasis has been devoted to the chemical composition and structure of clays. In fact, it is with a correct understanding of the structure-mediated properties that it is possible to maximize the valorization of this class of naturally occurring materials and find novel, alternative (and advanced) applications.

2. Chemical Composition and Structure-Property Relationship of Clays

As stated in the previous paragraph, clays are fine-grained 2D earthen minerals. In general, the chemical composition of earthen crust is mainly silica (ca. 60%) and alumina (ca. 15%) with other mineral oxides constituting the residual fraction (approximately 25%) [2]. Hence, the chemical composition of clays reflects the Earth's crust, since clays are hydrous alumino-silicates (eventually containing some minor impurities, i.e., Na, K, Mg, Ca, Fe) [1,2]. Clays are made up of layered sheets organized as follows:

(i) 2D 1-1 layered clay minerals, formed by alternating layers made by one tetrahedral (Si-based) sheet and one octahedral (Al-based) sheet held together by hydrogen bonding [2,64].

(ii) 2D 2-1 layered clay minerals (organized into six subgroups), formed by alternating layers made by two tetrahedral (Si-based) sheets sandwiching one octahedral (Al-based) sheet in the middle. These sandwich structures are held together by an interlayer made by either water molecules or exchangeable cations (to maintain the electroneutrality of the system), or even both [2,64].

An extended classification of clays based on their chemical composition, structural stacking, and interlayer organization is summarized in Figure 1 [2]. In detail:

(i) Kaolinite-serpentine subgroup: 1-1 layered structures: This subgroup is characterized by electroneutral layered structures and the absence of cations at the interlayer (with very low CEC, 3–15 cmol/kg). In particular, surface charges of kaolinite derived from the presence of defects (such as isomorphic substitution and broken edges Al-O-Al and Si-O-Si). Tetrahedral and octahedral sheets are held together by either secondary forces (e.g., hydrogen bonding) or water molecules. The kaolinite-serpentine subgroup is characterized by the general chemical formulas $Al_2Si_2O_5(OH)_4$ (for the kaolinite subgroup) and $Mg_3Si_2O_5(OH)_4$ (for the serpentine subgroup) [65]. Examples of clays belonging to this subgroup are kaolinite, halloysite, dickite, nacrite, crysotile, antigorite, lizardite (the latter three belonging to the serpentine subgroup).

(i) Pyrophyllite-talc subgroup: 2-1 layered structures: This subgroup is characterized by electroneutral layered structures and the absence of cations at the interlayer (with very low CEC, below 1 cmol/kg). Weak secondary forces (e.g., van der Waals and/or dipolar interactions) that favor a loss of cohesion between the layers hold tetrahedral sheets together. The pyrophyllite-talc subgroup is characterized by the general chemical formulas $Al_2Si_4O_{10}(OH)_2$ (for the pyrophyllite subgroup) and $Mg_3Si_4O_{10}(OH)_2$ (for the talc subgroup) [66].

(ii) Smectite subgroup: 2-1 layered structures: This subgroup is characterized by having octahedral sheets partially substituted, thus generating weak negatively charged layers. In order to balance such negative charge and maintain the electroneutrality of the system, the smectites interlayer region contains miscellaneous cations, together with water molecules. The presence of such an interlayer (made by water molecules and cations) enhances the water affinity of smectites, thus favoring the hydraulic delamination and expansion. Furthermore, smectites show a high ion exchange capacity (i.e., CEC approximately 70–100 cmol/kg). The smectite subgroup is characterized by the chemical formula $(Na,Ca)_{0.33}(Al,Mg,Fe,Zn)_2Si_4O_{10}(OH)_2 \cdot nH_2O$ [67]. Examples of clays belonging to this subgroup are: montomorillonite, beidellite, laponite, saponite, and hectorite.

(iii) Vermiculite subgroup: 2-1 layered structures. This subgroup is characterized by having both tetrahedral and octahedral sheets partially substituted, thus generating a net negative charge in both layers. In order to balance such net negative charge and maintain the electroneutrality of the system, the vermiculites interlayer region contains two oriented water layers and magnesium cations, thus providing a limited expansion capacity and high ion exchange capacity (i.e., CEC approximately 100–150 cmol/kg). The vermiculite subgroup is characterized by the chemical formula $(Mg,Ca)_{0.3}(Mg,Fe)_3(Si,Al)_4O_{10}(OH)_2 \cdot 4H_2O$ [68].

(iv) Mica subgroup: 2-1 layered structures: This subgroup is characterized by having the Si-based tetrahedral sheets partially substituted by aluminum atoms, thus generating a charge deficiency in the tetrahedral layers. In order to balance such strong negative charge and maintain the electroneutrality of the system, the micas interlayer region contains potassium cations occupying fixed positions at the tetrahedral sites surface. Such locked structure significantly limits the entry of water and micas ion exchange capacity (i.e., CEC approximately 10–40 cmol/kg). The mica subgroup is characterized by the chemical formula $(K,H)Al_2(Si,Al)_4O_{10}(OH)_2 \cdot nH_2O$ [69]. Examples of clays belonging to this subgroup are: muskovite, sericite, illite, biotite, and glauconite.

(v) Chlorites subgroup: 2-1 layered structures: This subgroup is characterized by having both tetrahedral and octahedral sheets partially substituted. In order to balance such negative charge and maintain the electroneutrality of the system, the chlorites interlayer region is made by hydroxide sheets, mainly constituted by brucite $Mg(OH)_2$, eventually partially substituted by iron atoms. The presence of hydroxyl functionalities at the interface between tetrahedral sheets and hydroxide-based interlayers induces the formation of hydrogen bonding that hold together the layered structures, generating a locked system characterized by having a poor ion exchange capacity (analogously as in the case of mica subgroup, namely: CEC approximately 10–40 cmol/kg). The chlorite subgroup is characterized by the chemical formula $(Mg,Fe)_3(Si,Al)_4O_{10}(OH)_2 \cdot ((Mg,Fe)_3(OH)_6)$ [70].

(vi) Inverted ribbons (palygorskite-sepiolite) subgroup: 2-1 layered structures: This subgroup is characterized by ribbons of 2-1 layered silicates presenting a periodic inversion of the apical oxygen atom in tetrahedral layers extending parallel to the layer directions, forming fibrous clays. These complex structures are characterized by the presence of nanometric channels (parallel-oriented respect to the direction of the layers) containing water molecules weakly bound to the magnesium ions forming the octahedral layers. The presence of these nanochannels guarantees high surface area (SSA higher than approximately 140–320 m^2/g) that allows their use as porous systems

for advanced applications (e.g, controlled transport and/or release of chemicals, drug-delivery, separation science) [71]. The chemical formulas of palygorskite-sepiolite subgroup are the following, namely: $(Mg,Al)_2Si_4O_{10}OH{\cdot}4H_2O$ (for the palygorskite subgroup), and $Mg_4Si_6O_{15}(OH)_2{\cdot}6H_2O$, (for the sepiolite subgroup) [72,73].

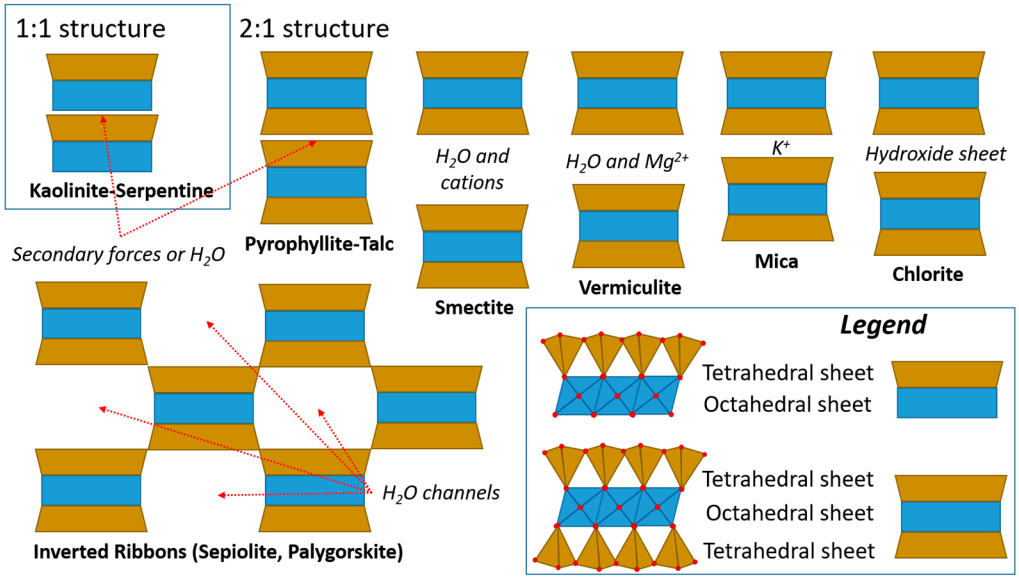

Figure 1. Schematic representation of 1:1 (inset) and 2:1 clay structures with a classification of the different subgroups of clays based on their stacking sequences. The difference in term of interlayers distance between the different subgroups of clays is comparable with the real one and depends on the species involved at the interface between the layered units. Reprinted with permission from [2]. Copyright 2018 IOP Publishing.

Furthermore, mixed-layer clays are also available in nature, but for the sake of simplicity, they are not discussed in this document (for details concerning mixed-layer clays, please refers to the following references [74,75]).

Clays belong to the ceramic materials class, characterized by having a crystalline organization with strong bonds (i.e., covalent bonds, and ionic bonds) between atoms forming the layers and secondary bonding (i.e., van der Waals forces, H-bonds) between the layers [2]. This particular architecture indicates a certain level of anisotropy in clays that exhibit cleavage subjected to forces applied parallel respect to the layer direction (thus, acting against the secondary bonding). Furthermore, as previously discussed, clays are characterized by having different chemical species at the interlayer that can somehow exert a different attraction between layers. In fact, depending on the chemical species at the interlayer, clays have different CEC, interlayer thickness (and consequently surface area), and hydration/gel-forming capacity. In detail:

(i) Cation exchange capacity (CEC): The CEC corresponds to the amount of cations (expressed in cmol/kg) that can be exchanged with other cations at the surface of clays. The CEC is influenced by the nature and amount of cations at the clays interlayer.
(ii) Interlayer thickness: Depending on the chemical species forming the interlayer, these generate different electrostatic forces (and consequently different degree of attraction) between the different sheets forming the layer structures of clays. These electrostatic forces influence the interlayer thickness.
(iii) Hydration/gel-forming (or swelling) capacity: Mechanisms at the basis of hydration are mostly two: (a) electrical properties of both clay's inorganic surface and aqueous medium affecting the water molecules orientation at the clay's surface, and (b) osmosis. Furthermore, both hydration and swelling properties are strongly affected by the nature and the quantity of exchangeable cations present at the interlayer, and these

values can be predicted considering the hydration energy of the different ions. In fact, the swelling capability follows the order: Mg > Ca > Li > Na > K [2].

Typical values of CEC, interlayer thickness, specific surface area, and swelling capacity of the different clay subgroups are summarized in Table 1 [2,76].

Table 1. Properties of the different subgroups of clays [2,7,76].

Clays Subgroups	CEC (cmol/kg)	Interlayer Thickness (Å)	Specific Surface Area (m^2/g)	Swelling Capacity
Kaolinite-Serpentine	3–15	7	5–40	None
Pyrophyllite-Talc	<1	9	5–40	None
Smectite	70–100	10–11	40–800	High
Vermiculite	100–150	12–15	500–700	High
Mica	10–40	10–11	50–200	Low
Chlorites	10–40	12–15	10–60	None

3. Advanced Applications: The Second (Technological) Life of Clays

As previously introduced, the peculiar properties of clays are the basis of the evolution (or better, the revolution) around this class of materials, going from being the simplest and oldest material handled and modeled by humans toward being still an important protagonist in the more attractive brand new technologies of the new millennium. In order to provide a detailed discussion on the advanced uses of clays in new technologies, the following paragraphs discuss the most catching eye technologies and case studies involving clays.

3.1. Biomedical Applications

Mousa and coworkers [7] point out that clay surface reactivity (due to CEC, ionic species at the interlayers, surface area and sorption capacity) is of paramount relevance for the biomedical interaction toward living tissues and fluids and synthetic prosthetic devices. In particular, clays are typically included in polymeric matrices to form both soft functional biocompatible scaffolds, hydrogels, and physical gels with improved mechanical responses [77], and hard porous scaffolds and sponges mimicking the bone tissue structural organization [78]. In this context, Giannelli et al. [5] produced a hard composite scaffold made by a keratin 3D sponge matrix, with magnetic Mg/Fe-hydrotalcite nanoparticles dispersed as fillers. These magnetic nanoparticles are able to stimulate the cell adhesion and proliferation by applying an external magnetic field. Results showed that the application of an external magnetic stimulus facilitates the cell proliferation, thus confirming the fundamental role of the magnetic clay component in the biomedical device. Furthermore, these systems show enhanced biocompatibility with osteoblasts and fibroblasts cells. Another interesting study is the one by Cui and coworkers [6], where a microporous 3D hydrogel made by modified chitosan and montmorillonite to promote tissue regeneration was developed. In this composite system, clays play a fundamental role in both increasing the mechanical properties of the hydrogel and improving the final interconnected microstructure. Results indicate the clay-induced microporous structure promotes the native cell infiltration, proliferation, and spontaneous differentiation without including growth factor and drugs in the formulation.

Murugesan et al. [8] critically analyzed the most recent literature describing the development of clay-based nanocomposites for biomedical applications. In particular, clay-containing nanocomposites under the shape of thin films are mostly used as drug-delivery patches, biodegradable/biocompatible packaging films, and microfluidic systems. These thin films are mostly produced following the fabrication techniques used in the field of nanocomposites such as solution blending, melt mixing, electrospinning, in situ polymerization [8]. In this process, both clays and polymers are dissolved in a common solvent (eventually, the two dispersions/solutions are separately prepared and added together), and transferred in the desired mold (i.e., solution blending) or deposited (i.e., cast

films). Vice versa, the melt intercalation passes through the dispersion of the clays within the molten polymer. Alternatively, the in situ intercalative polymerization requires the dispersion of clays in a monomer solution and subsequently let the monomers polymerize by applying an external stimulus. The advantages of producing thin films are mostly in terms of chemical and mechanical resistance (compared to different morphologies).

Another interesting technology applied to clays is their integration into polymeric matrices to produce fibers, drug-delivery patches, or fiber-based membranes/scaffolds fabricated via electrospinning. In this case, clays are firstly dispersed in the polymer/solution, letting the clay-containing mixture pass through a needle spinneret and finally deposited onto the substrate pushed by the charge difference between the needle and the collector. The fiber morphology is driven by several parameters such as voltage intensity, the working distance between the needle and the collector, and the geometry of the needle [8,79]. In these fiber-based systems, the role of clays is to enhance the mechanical performance and the thermal stability of the composite, also improving the processability. In the study by Hong and coworkers [80], an organically modified montmorillonite prepared by a solution intercalation method in the presence of polyurethane was successfully deposited via electrospinning, producing a nanocomposite with 200%-enhanced mechanical response (both in terms of Young modulus and tensile strength) with respect to the base polymer.

The production of suitable bioinks for 3D printing and biofabrication passes through several printing methods (e.g., inkjet, extrusion, laser-assisted printing) [81,82]. The details concerning 3D printing technologies are provided in the dedicated following paragraph. However, for the sake of completeness, the biomedical applications involving bioprinting of clay-based systems are discussed here. Bioprinting consists of producing scaffolds or tissues via additive manufacturing (i.e., typically extrusion-based printing). These tissues/scaffolds are made by cells included in a host matrix (mostly biopolymers or hydrogels). One of the main concerns related to these very complex formulations (borderline between living organism and unanimated matter) is the rheology of the system that should be perfect (i.e., not too much as it can cause mechanical stresses to the cells, not too low as the final formulation should be printable and maintain the desired shape). In this context, nanoscopic clays (nanoclays) can be a very efficient and effective additive for such type of bioinks since they enhance the mechanical strength and viscosity of the system, maintaining the final shape, showing high processability and enhancing the biological activity [8]. Furthermore, the formulations containing nanoclays can be stimuli-responsive toward electrical, temperature, and pH variation, making these systems very appealing for muscular tissue regeneration [83–85]. A clear example of these stimuli-responsive systems is the study by Guo et al. [86] where an agarose/polyacrylamide-based thermo-responsive hydrogel containing laponite (which is a synthetic clay belonging to the smectite subgroup) has been successfully prepared and tested. In this particular formulation, clays increase the processability, the post-printing stability, and the final mechanical properties with respect to the bare agarose/polyacrylamide hydrogels.

As previously introduced, clays are characterized by a particular particle size, porosity and surface area, and reactivity coupled with their biocompatibility that allow their use in drug-delivery systems, in pharmaceutical applications, and in cancer research, diagnosis and relative therapy [9,87]. In particular, nanoclays are exploitable as nanoscopic carriers for the delivery of anticancer drugs directly to the tumor site. Furthermore, several in vitro and in vivo tests highighted that nanoclays show bioactivity against different cancers ([9,88] and references therein). This is, for instance, the case of bentonite that inhibits the growth of central nervous system (glioblastoma) cells, while enhancing the growth of lung adenocarcinoma cells [88]. Interestingly, a montomorillonite/palygorskite clay mixture significantly reduces melanoma cell proliferation and viability by in vitro tests, and melanoma growth in an in vivo animal model by inducing a reduction of the tumor size and weight, decreasing tumor cell mitosis, and inducing tumor necrosis [89]. Nanoclays are used (in combination with polymeric and/or magnetic nanoparticles) to transport specific anticancer drugs directly to the tumor site. This is, for instance, the case of the study by

Lin and coworkers [90] where a Na-montmorillonite was loaded with 5-fluorouracil (a drug used in the colorectal cancer therapy) but reaching the maximum loading capacity of only 2 wt.%. To increase the loading capacity of montmorillonite, montmorillonite was amino-modified and grafted with β-cyclodextrin, reaching a higher 5-fluorouracil loading of approximately 28 wt.% [91]. However, Peixoto et al. [9] classified the use of clays in oncologic therapy against different types of cancer depending on the target organ/apparatus, namely lung, colorectal, gastric, breast, pancreatic, brain, skin, thyroid, and bone cancer. For all these cases, clays are used as carriers of bioactive chemicals, either directly as they are or after a surface functionalization (as depicted in Figure 2) [92].

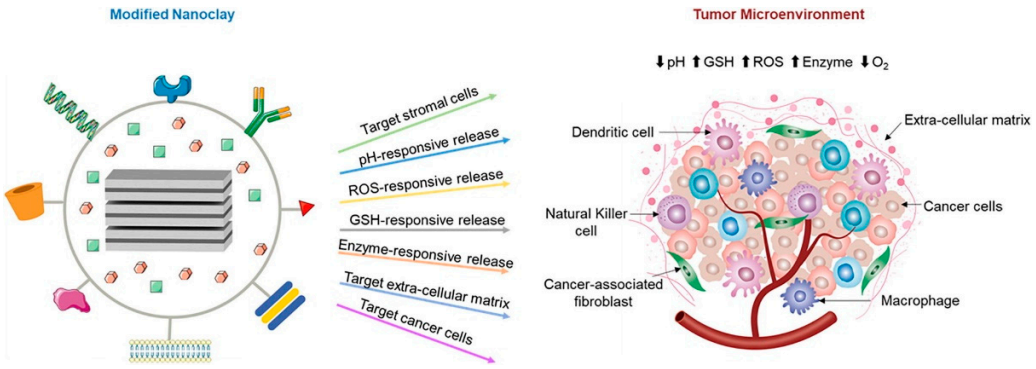

Figure 2. Schematic illustration of strategies used to expand the functions of nanoclays. The modified-nanoclays target the tumor microenvironment (TME), increasing the efficacy of cancer therapy. TME has been shown to have different characteristics from normal tissues, which can be vascular defects, higher expression of given enzymes, elevated glutathione (GSH), hydrogen ion, and reactive oxygen species (ROS) concentrations. Reprinted with permission from [9]. Copyright 2021 Elsevier B.V.

In general, most of the cases investigated used mostly halloysite nanotubes (HNTs), but also montmorillonite, bentonite, laponite, palygorskite, and kaolinite. Figure 3 reports the mechanism involving the pH- and time-responsive release of an anticancer drug loaded by HNTs, delivered through oral administration. As reported by the authors, the role of HNTs (i.e., clays) within this technological approach is very appealing as it minimizes the undesired (early) drug release in the stomach, whereas it maximizes the drug release directly in the intestines, the site affected by the colorectal cancer [9].

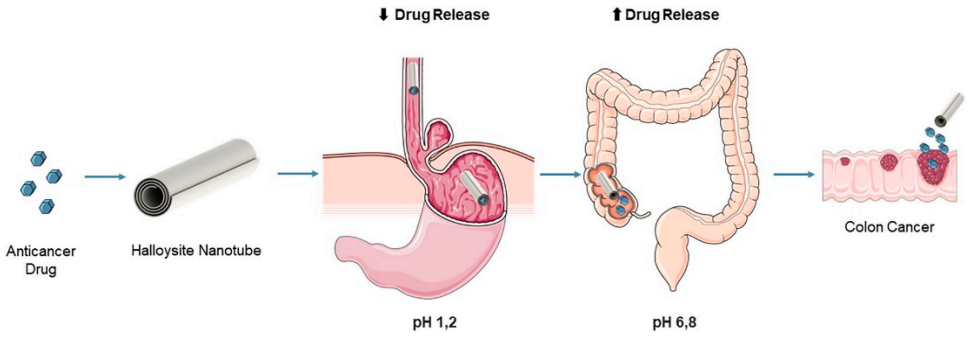

Figure 3. Schematic illustration of a pH-responsive nanoclay system for anticancer drug delivery to the intestines, avoiding early release in the stomach. Reprinted with permission from [9]. Copyright 2021 Elsevier B.V.

Furthermore, these systems are exploitable in diagnostics by simply loading/grafting specific biomarkers or magnetic nanoparticles that can detect the presence of cancer cells in the organism [93,94]. For a detailed study of the diagnostics and imaging of pathological alterations in living systems, please refer to [95].

3.2. Environmental Applications

The continuous depletion of freshwater resources is one of the main concerns affecting the social and economic progress of several underdeveloped areas of Third and Fourth World countries [2]. To overcome this issue, probably the best technological solution is to significantly increase the recyclability of polluted (waste)water into newly clean drinkable water [96,97]. In this context, the scientific literature proposes several alternative approaches for the abatement of anthropogenic (in)organic pollutants from contaminated (waste)water [98–108]. Historically, the use of soil-matter, sand, gravel, and stone as water filtering materials dates back to the Egyptian and ancient Greeks periods [109]. The scientific awareness of the contemporary society pointed out that fundamental parameters influencing the sorption capacity of materials are the surface area and charge, pore volume, and the presence of specific reactive species available at both surface and interface [2,110]. Due to their particular morphological characteristic and related properties, clays represent a very promising class of nanomaterials exploitable in contaminated freshwater and wastewater clean-up processes.

Based on the literature analysis proposed by Uddin [11], clays are effective adsorbents for the removal of heavy metal ions (i.e., As, Cd, Co, Cr, Cu, Hg, Mn, Ni, Pb, Zn) from aqueous solutions, mostly due to their specific surface area and capability of ion exchange (i.e., CEC). In particular, the majority of clays are negative charged with positive cations present at the interface/surface, and available for interacting with metal cations present in a solution following different mechanisms (i.e., mostly ion exchange, but also direct bonding between adsorbent surface and adsorbate species, complexation, and many others). Furthermore, clays can be modified in order to enhance their sorption capacity (e.g., by varying the hydrophilicity/hydrophobicity degree of the surface and by introducing some novel chemical functionalities). In particular, some scientific studies show the importance of both solution pH and thermal treatment (performed on clays) over the adsorption mechanism [11,111–115]. In fact, experimental evidences highlight that the sorption of As(V) over a mixture of different natural clays is maximized at acid conditions [111]. However, in the case of Cr(VI), Cu(II), and Zn(II), an optimum sorption pH at approximately circumneutral conditions [112,113] has been registered. The explanation of this phenomenon is not trivial and depends on both the nature of the clays and heavy metal cations. The literature proposes that pH variations strongly affect the availability of ionic species and the competition for adsorption sites, also influencing the chemical precipitation of metal ions as hydroxyl species [11,114]. Concerning the effect of the thermal pretreatment over clays sorption capacity, even here the trend is still unclear. There is evidence that the sorption capacity is maximized along with the thermal treatment (this is, for instance, the case of Cr(VI) sorption over a 200 °C fired clay) [115]. On the contrary, there is also some evidence that the clay sorption capacity is reduced after firing at higher temperature (and this is the case of the same cation Cr(VI) over a 400 °C fired clay, for details please refer to [11] and references therein). Es-Sahbany and coworkers [15] reported the use of a clay mixture extracted from a Morocco region made by kaolinite, illite, quartz, and traces of vermiculite, showing an overall CEC value of approximately 27 meq/100 g and a pH of 8.8. This mixture was tested for the sorption of heavy metals, namely Co(II), Cu(II), Ni(II), and Pb(II). Experimental results showed the maximum abatement (elimination yield ca. 85%) for all these cations was reached at alkali pH (approximately 8.0–8.5) with a contact time of approximately 90 min [15].

In many cases, modification treatments are proposed as technical solutions to significantly enhance clay sorption performances. Peralta et al. [10] reported the preparation of magnetic clays by introducing magnetic nanoparticles by different mechanisms, namely at the interlayer, within the porous channels, by direct interaction with the siloxane functional groups at the surface/edge of the mineral clay, thus forming magnetic nanocomposites [10,116]. Furthermore, the introduction of a magnet-sensitive fraction is very appealing as it can substantially favor the recovery of the nanocomposites by simply applying an external magnetic stimulus [117–119]. In particular, Peralta and coworkers [10] reported

that the typical routes to prepare such magnetic nanocomposites are: coprecipitation, intercalation, and pillaring. Figure 4 reports the main relevant mechanisms [10]. These methods are:

(i) Pillaring: This method consists of introducing a pillar within the structure of the clay by permanently stacking the interlayers, generating a higher porosity [120]. Pillaring is mostly a cationic exchange method in which inorganic species are introduced within the interlayer of clays forming robust oxides strongly bound to the layers of the minerals [17]. In this specific context, the mechanisms proposed are two: either the incorporation of magnetic nanoparticles within the pores of the pillared clays (Figure 4, route A1) or using the magnetic nanoparticles as pillars to expand the interlayer distance of the clays (Figure 4, route A2) [10].

(ii) Coprecipitation: This method consists of the in situ formation of magnetic nanoparticles [121] by performing the synthesis directly in an aqueous dispersion of clays (Figure 4, route B).

(iii) Intercalation: This method consists in the physical insertion of target chemical species within the interlayers/pores of the clays [122]. In this specific context, the mechanisms proposed are two: either the inclusion of magnetic nanoparticles within a previously surfactants-intercalated clay to facilitate the entrance of the magnetic nanoparticles (Figure 4, route C1) or the direct intercalation of surfactant-stabilized magnetic nanoparticles (Figure 4, route C2) [10].

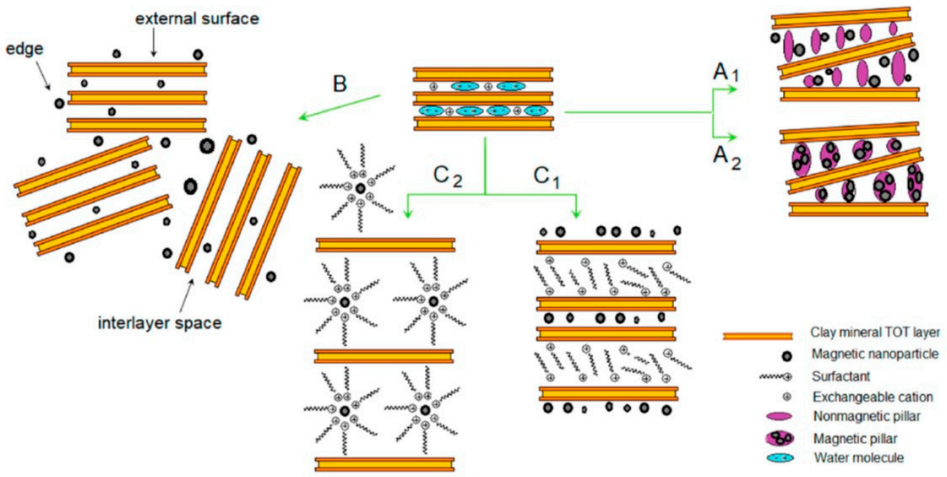

Figure 4. Schematic illustration of typical synthesis routes to obtain magnetic nanoparticles/clay minerals 2:1 type nanocomposites: (A1) pillaring with nonmagnetic pillar; (A2) pillaring with magnetic pillar; (B) coprecipitation route; (C1) intercalation of magnetic nanoparticles into a surfactant intercalated clay; (C2) intercalation of a surfactant-modified magnetic nanoparticles into a clay. Reprinted with permission from [10]. Copyright 2020 MDPI.

In this context, Magdy et al. [123] prepared a kaolinite magnetic nanocomposite via coprecipitation and successfully tested it for the abatement of an anionic dye (Direct Red 23) at neutral pH, reaching the maximum adsorbent capacity of approximately 23 mg/g.

Mukhopadhyay et al. [12], instead, investigated the inorganic modification of two different types of clays, namely smectite and kaolinite, for the adsorption of As(V). In particular, three modified clays were prepared, namely Fe-exchanged smectite, Ti-pillared smectite, and phosphate-bond kaolinite, and results were compared with the bare unmodified clays. Results indicated that these modifications influenced the clays' pH, specific surface area, and CEC. Concerning smectite, both Fe-exchange and Ti-pillaring cause a reduction of the pH (from ca. 8.0 to ca. 4.0–6.0) mainly due to the saturation of the clay sites, a consequent decrement of the CEC since these reactions blocked the availability of sorption sites and increment of the specific surface area (from ca. 200 m^2/g up to 440–480 m^2/g). Concerning kaolinite, instead, phosphate-bonding causes a negligible

pH variation, a double increment of the CEC due to ligand adsorption, and a remarkable increment of the specific surface area (from ca. 18 m^2/g up to ca. 90 m^2/g). Results indicate that all these modification significantly better the sorption performances with respect to the bare reference clays [12].

Interestingly, clays might be helpful in advanced oxidation processes (AOPs), which are a very promising category of methods for the removal of organic pollutants present in water by radical-mediated oxidation reactions in most cases light-mediated (i.e., photocatalysis) [124–128]. Heterogeneous AOPs required the use of a semiconductor capable of generating radical species once activated by UV/visible light radiation (i.e., photocatalyst). The most studied semiconductors for this application are TiO_2 (mostly anatase phase) [129], ZnO [130] and iron oxides (for photo-Fenton and Fenton processes) [117,131,132]. In particular, clays might be used as either a simple substrate for the delivery of the semiconductors or chemical functionalized to produce a new heterostructure working directly as a photocatalyst. In this context, Akkari et al. [14] developed different ZnO-sepiolite heterostructures and successfully tested them as photocatalysts for the degradation of an aqueous solution contaminated by several anthropogenic pharmaceuticals, taken as model emerging pollutants. Baloyi et al. [17], instead, analyzed the most recent scientific literature describing the use of pillared clays in heterogeneous AOPs for water purification.

Furthermore, concerning the more traditional possibility of using clays as sorbing materials, Azzam et al. [133] reported the treatment of olive mills wastewater (rich in phenols and other organic compounds) by using a mixture containing muscovite and albite, registering a reduction of the chemical oxygen demand (COD below 40%) and phenols concentration (below 80%). Li et al. [16] reported the performances of montmorillonite, kaolinite, and palygorskite in the abatement of a cationic dye (i.e., Rhodamine 6G). Results showed that nonswelling clays (i.e., kaolinite and palygorskite) show a relatively low dye uptake (below 140 mmol/kg) if compared to swelling clay (i.e., montomorillonite, 785 mmol/kg). The rationalization of this behavior is due to the important role of the interlayers (which is available in the case of the swelling clay) in the sorption mechanism.

Sometimes, it is necessary to induce a higher affinity between the inorganic clays and hydrophobic organic species present in the aqueous medium. To do this, researchers investigated the possibility of surface functionalize clays by substituting the interlayer cations with either organocations or covalently-bonded organic moieties, thus generating organoclays [134]. Among clays, smectites, (primarily montmorillonite) have been extensively used to prepare organoclays because of their high CEC, swelling behavior, sorption properties, and large surface area [134]. Other organoclays rely on micas, hectorites, and sepiolites. Organoclays are mostly prepared in solutions by means of either cation exchange reaction or by solid-state reaction. These methods are:

(i) Cation exchange reaction: This method consists of exchanging the interlayers cations with quaternary alkylammonium cations in aqueous solution.
(ii) Solid-state reaction: This method consists of intercalating organic molecules in dried clays (i.e., in absence of solvents).

Depending on the hydrophobic chain length, it is registered an increment of the structural ordering along with the increment of the chain length (as depicted in Figure 5) [135].

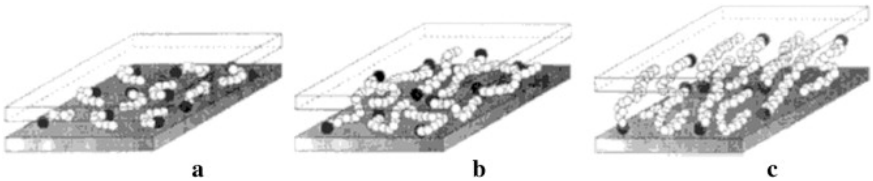

Figure 5. Schematic illustration of chains aggregation models in alkyl-modified organoclays: (**a**) short chains length, lateral monolayer; (**b**) medium chains length, in-plane disorder and interdigitation to form quasi bilayers; (**c**) long chains length: interlayer order increases leading to a liquid–crystalline polymer environment. Reprinted with permission from [135]. Copyright 1994 American Chemical Society.

As reported by Beall et al. [13], organoclays interact against organic contaminants by partitioning them within their hydrophobic layer, which acts as a real organic phase. The efficiency of these systems is driven by the solubility of the target organic pollutant in the water medium and its affinity toward the organic phase in the organoclays channels. One of the main industrial applications of these organoclays is in the recovery of acid emulsified oil well fluids from petroleum offshore platforms [13].

Lastly, further steps forward have been realized in the structural use of clays for the development of advanced ceramic membranes for water purification [19–22]. In this context, it should be noted that the use of a well-consolidated technology such as membrane separation surely guarantees industrial feasibility and speeds up its integration in a productive process. As reported by Abdullayev et al. [19], membranes can be divided into polymeric membranes (cheap, but poor stable) and ceramic ones (expensive, but highly stable). To reduce the costs of ceramic membranes, over the past few years there has been increasing interest in the use of low-cost clays as precursors for the fabrication of cheap (but effective) ceramic membranes. Among these, kaolinite is the most preferred clay used to fabricate ceramic membranes for the relatively low thermal processing and sintering conditions required. Other clays exploited for the fabrication of ceramic membranes are bentonite, sepiolite, and attapulgite [19]. Rashad and coworkers [20] investigated the fabrication of a mullite membrane for microfiltration of oil-in-water emulsion. Results indicated that this system showed an excellent pH stability (from acid to alkaline), high oil rejection, and high regularity in terms of pore size distribution and surface roughness. Elgamouz et al. [21], instead, evaluated the possibility of producing a porous ceramic membrane from a mixture of clays recovered from a particular region of Morocco. Subsequently, the authors modified the clays' porous substrate by further hydrothermal deposition of a templated silicalite coating obtained via sol-gel. Permeability tests against three different gases (namely, N_2, C_3H_8 and SF_6) showed that these membranes have high selectivity with respect to SF_6 relative to N_2, whereas they are hardly selective for C_3H_8. Abubakar et al. [22], instead, exploited a mixture of clays (rich in kaolinite and illite) from a Nigerian mine to fabricate a porous membrane (average pore diameter ca. 5–6 nm). In particular, after sintering at 1300 °C for 2 h, mullite ($3Al_2O_3{\cdot}2SiO_2$, obtained by calcination of kaolinite) and cristobalite (a polymorph of quartz) were formed. The resulting membranes were successfully tested in the separation of U from an aqueous medium, thus simulating the remediation of U-containing wastewaters deriving from fracking, oil exploration, and phosphate mining industries. Foorginezhad et al. [136] produced microfiltration membranes from nanoscopic clays via dry pressing in the presence of natural zeolites and tested these ceramic membranes against cationic and anionic dyes from contaminated water. Due to the negative charge of the clay-membrane, high removal efficiencies are reached for the positively charged species rather than for the negatively ones.

3.3. Other Advanced Applications: Additive Manufacturing and Sol-Gel Processes

Additive manufacturing (AM, also known as either rapid prototyping, or more commonly 3D-printing) is a class of processes extremely useful for obtaining three-dimensional objects starting from a 3D model (by means of a Computer Aided Design, or CAD model) and forming them by depositing layer upon layer [137–140]. Most diffused AM processes are fused deposition modelling (FDM), direct metal laser sintering (DMLS), selective laser melting (SLM), and electron beam melting (EBM) [141–144]. According to the literature, AM processes are exploitable for producing metals [145], polymers [146], ceramics [147], composites and concretes [148,149], carbonaceous materials [137], hydrogels [150], biomaterials [151], engineered tissue and organs [152,153], and food [154]. In this context, clays may also be used in AM to properly manufacture valuable objects.

Chen and coworkers [155] investigated the cement 3D printability by introducing into the formulation ca. 60 wt.% low-grade calcined clay (mainly made by metakaolin), ca. 30 wt.% limestone, and ca. 2 wt.% admixtures (such as plasticizers and/or viscosity modifiers). By increasing the content in clays, it registered a significant reduction of slump,

flowability and initial material flow rate. Moreover, results pointed out a buildability improvement (caused by reduced water film thickness), an acceleration of the initial setting and stiffness, together with an increment of the specific surface area. For the sake of comparison, a reduction of the compressive strength due to the dilution effect exerted by the cementitious fraction replacement was also noted. Another interesting study focused on the introduction of calcined clays in cementitious formulation for 3D printing is the one written by Long et al. [156]. The authors registered a significant improvement of several mechanical parameters (i.e., dynamic yield stress, static yield stress), structural recovery, and shape retention during printing of the final mortar containing a 33.33 wt.% in calcined clays. Faksawat and coworkers [157] investigated the possibility of producing composite paste (for future bone-replacement orthopedic implants) made by raw clays and hydroxyapatite (at different ratios from 95:5 to 75:25) by FDM 3D printing. Chikkangoudar et al. [158], instead, evaluated the effects of adding nanoclays in polypropylene filaments for 3D printing, registering an enhancement of the filament dimensional flexibility and a reduction of the deformation of the 3D printed models (counterbalanced by an increment in fragility affecting both filaments and 3D printed models by increasing the nanoclays content). For completeness, case studies discussing the introduction of clays into formulation for 3D printing of biomedical devices are already discussed in the previous paragraph dedicated to the biomedical applications.

Sol-gel process represents a bottom-up procedure to produce ceramic metal oxides under the shape of particles, films, fibers, gels (i.e., xerogels, cryogels, aerogels), and monoliths [159–166]. This technique consists of a series of (acid/alkaline catalyzed) in situ polycondensation reactions involving monomers (i.e., metal oxides precursors), and converting them from a colloidal solution (sol) into an integrated network (gel) [161]. In the previous paragraph, we reported that the surface sites of clays are important sites for further functionalization and grafting. It is also possible to disperse clays in a proper medium in the presence of the selected oxide precursor and directly fabricate a nanocomposite through a sol-gel polymerization mechanism. Meera et al. [35] reported the preparation of silica-(organo-modified) montmorillonite nanocomposites in aqueous medium via a direct sol-gel process. Results showed that the presence of the clay fraction influenced the final morphology of the nanocomposite, and increased the surface hydrophobicity, conferring anti-wetting properties. Furthermore, clays also increased the thermal stability of the nanocomposite (with a shift of ca. 40 °C). In Qian et al. [34], the authors produced a silica-montmorilllonite composite registering the formation of mesoporous silica nanostructures covering the clay surface. Results indicate that acid-catalyzed systems show large continuous mesoporous silica covering the clay surfaces, with a substantial increment of the surface area (from ca. 30 m^2/g to ca. 560 m^2/g). In noncatalyzed systems, the morphology is a bit different as silica nanoparticles result being attached on 2D clay platelets, and the increment in the surface area is contained (from ca. 30 m^2/g to ca. 165 m^2/g). The comparison between the two different mechanisms is sketched in Figure 6 [34].

Coming back to the environmental applications, Pronina et al. [167] reported the deposition of different porous titania coatings (sol-gel mediated) onto expanded clays, and their integration into fluidized-bed photocatalytic reactors. These nanocomposites were successfully tested in the photocatalytic abatement of tetracycline antibiotics from aqueous solutions. Results showed a synergy between clay and titania as the degradation mechanism were a combination between adsorption and photocatalytic abatement.

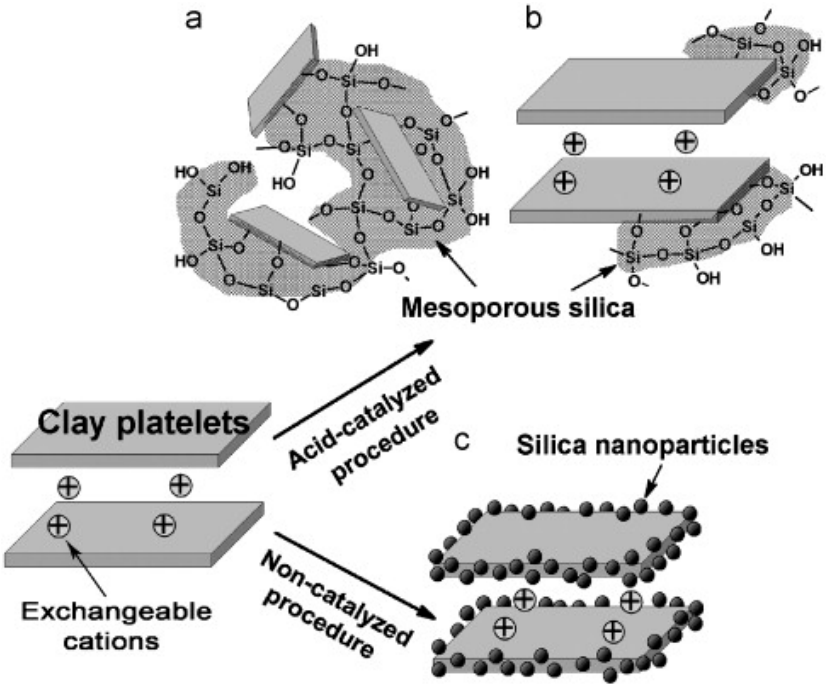

Figure 6. Schematic representation of the proposed structural models for the sol-gel-modified clays in the case of acid-catalyzed procedures: (**a**) a cross-linked structure at high TEOS/clay ratio; (**b**) mesoporous silica attached on clay surface at low TEOS/clay ratio, and in the case of non-catalyzed procedures: (**c**) silica nanoparticles attached on clay surfaces. Reprinted with permission from [34]. Copyright 2008 Elsevier B.V.

4. Conclusions and Future Perspectives

Clays are 2D layered hydrous alumino-silicates extracted from earth. This extremely varied class of materials has been exploited since ancient times for preparing traditional ceramics, such as earthenware, stoneware, porcelains, potteries. It is with the increased scientific awareness of the modern era that some interesting structure-property relationships of clays emerged as a very peculiar characteristic of this class of materials. In particular, what is quite surprising is the continuous interest that even nowadays surrounds clays that result still being appealing for a plethora of novel advanced technological applications, very far from the production of traditional ceramics.

However, the large multitude of different applications in most cases does not facilitate understanding the chemistry behind clays. This is mainly due to the fact that the majority of the review documents found in the scientific literature are primarily focused on the applications, not on the materials. Therefore, with this document, this author hopes to have finally filled this gap. In particular, after providing an economic analysis of the global trading of clays, the text has been organized into two main sections. Part I is dedicated to the classification of clays based on their structural and chemical composition, together with a schematic summary of the main relevant structure-induced properties, which are strongly correlated to the nature and quantity of chemical species at the interlayer, CEC, interlayer thickness, surface area, and hydration/gel-forming capacity among the others. Part II, in contrast, is dedicated to the analysis of the nonconventional applications of clays in technological fields of emerging interest. In particular, several case studies describing the use of clays in biomedicine, environmental remediation, membrane technology, additive manufacturing, and sol-gel processes are presented, and experimental results are critically discussed and correlated with the clay structure-property relationship. In fact, a more correct comprehension of the mechanisms involved is the only way to maximize the valorization of this class of inorganic materials.

Therefore, at the end of this study, we clearly understand that the future of clays is still fluid and very promising. In particular, this author believes that the applications where clays can make the difference are the ones where their biocompatibility can play a pivotal role. For this reason, particular attention has been paid to the application fields such as biomedicine and environmental remediation of contaminated media. However, it should be highlighted that biocompatibility is a major property even considering the end-of-life fate of a given object. This last assumption confirms and encourages once again the growing attention that clays have attracted in the recent years.

Funding: This research received no external funding.

Institutional Review Board Statement: Not applicable.

Informed Consent Statement: Not applicable.

Data Availability Statement: Not applicable.

Acknowledgments: My interest in clays dates back some years, and the inspiration was an afternoon talk with my grandfather Giuseppe "Pino" Salerno (1933–2020) having object the "return to the earth" concept, meaning that the future of humanity passes through sustainability, agriculture, and saving the environment. His life of sacrifice between industry (in youth) and agriculture (his great passion and hobby) was always a model to me. Unfortunately, after a bad lymphoma broke out during the COVID pandemic, he died in April 2020. I think that the resulting manuscript fully respects his philosophy.

Conflicts of Interest: The author declares no conflict of interest.

References

1. Guggenheim, S.; Martin, R.T. Definition of clay and clay mineral: Joint report of the AIPEA and CMS Nomenclature Committees. *Clay Miner.* **1995**, *30*, 257–259. [CrossRef]
2. Nisticò, R. The importance of surfaces and interfaces in clays for water remediation processes. *Surf. Topogr. Metrol. Prop.* **2018**, *6*, 043001. [CrossRef]
3. Zou, Y.-C.; Mogg, L.; Clark, N.; Bacaksiz, C.; Milanovic, S.; Sreepal, V.; Hao, G.-P.; Wang, Y.-C.; Hopkinson, D.G.; Gorbachev, R.; et al. Ion exchange in atomically thin clays and micas. *Nat. Mater.* **2021**, *20*, 1677–1682. [CrossRef]
4. Yang, Y.; Liu, X.; Zhu, Z.; Zhong, Y.; Bando, Y.; Golberg, D.; Yao, J.; Wang, X. The role of geometric sites in 2D materials for energy storage. *Joule* **2018**, *2*, 1075–1094. [CrossRef]
5. Giannelli, M.; Barbalinardo, M.; Riminucci, A.; Belvedere, K.; Boccalon, E.; Sotgiu, G.; Corticelli, F.; Ruani, G.; Zamboni, R.; Aluigi, A.; et al. Magnetic keratic/hydrotalcites sponges as potential scaffolds for tissue regeneration. *Appl. Clay Sci.* **2021**, *297*, 106090. [CrossRef]
6. Cui, Z.-K.; Kim, S.; Baljon, J.J.; Wu, B.M.; Aghaloo, T.; Lee, M. Microporous methacrylated glycol chitosan-montmorillonite nanocomposite hydrogel for bone tissue engineering. *Nat. Commun.* **2019**, *10*, 3523. [CrossRef] [PubMed]
7. Mousa, M.; Evans, N.D.; Oreffo, R.O.C.; Dawson, J.I. Clay nanoparticles for regenerative medicine and biomaterial design: A review of clay bioactivity. *Biomaterials* **2018**, *159*, 204–214. [CrossRef] [PubMed]
8. Murugesan, S.; Scheibel, T. Copolymer/clay nanocomposites for biomedical applications. *Adv. Funct. Mater.* **2020**, *30*, 1908101. [CrossRef]
9. Peixoto, D.; Pereira, I.; Pereira-Silva, M.; Veiga, F.; Hamblin, M.R.; Lvov, Y.; Paiva-Santos, A.C. Emerging role of nanoclays in cancer research, diagnosis, and therapy. *Coord. Chem. Rev.* **2021**, *440*, 213956. [CrossRef]
10. Peralta, M.E.; Ocampo, S.; Funes, I.G.; Onaga Medina, F.; Parolo, M.E.; Carlos, L. Nanomaterials with tailored magnetic properties as adsorbents of organic pollutants from wastewaters. *Inorganics* **2020**, *8*, 24. [CrossRef]
11. Uddin, M.K. A review on the adsorption of heavy metals by clay minerals, with special focus on the past decade. *Chem. Eng. J.* **2017**, *308*, 438–462. [CrossRef]
12. Mukhopadhyay, R.; Manjaiah, K.M.; Datta, S.C.; Yadav, R.K.; Sarkar, B. Inorganically modified clay minerals: Preparation, characterization, and arsenic adsorption in contaminated water and soil. *Appl. Clay Sci.* **2017**, *147*, 1–10. [CrossRef]
13. Beall, G.W. The use of organo-clays in water treatment. *Appl. Clay Sci.* **2003**, *24*, 11–20. [CrossRef]
14. Akkari, M.; Aranda, P.; Belver, C.; Bedia, J.; Haj Amara, A.B.; Ruiz-Hitzky, E. Reprint of ZnO/sepiolite heterostructured materials for solar photocatalytic degradation of pharmaceuticals in wastewater. *Appl. Clay Sci.* **2018**, *160*, 3–8. [CrossRef]
15. Es-Sahbany, H.; Hsissou, R.; El Hachimi, M.L.; Allaoui, M.; Nkhili, S.; Elyoubi, M.S. Investigation of the adsorption of heavy metals (Cu, Co, Ni and Pb) in treatment synthetic wastewater using natural clay as a potential adsorbent (Sale-Marocco). *Mater. Today Proc.* **2021**, *45*, 7290–7298. [CrossRef]
16. Li, Z.; Potter, N.; Rasmussen, J.; Weng, J.; Lv, G. Removal of rhodamine 6G with different types of clay minerals. *Chemosphere* **2018**, *202*, 127–135. [CrossRef] [PubMed]

17. Baloyi, J.; Ntho, T.; Moma, J. Synthesis and application of pillared clay heterogeneous catalysts for wastewater treatment: A review. *RSC Adv.* **2018**, *8*, 5197–5211. [CrossRef]
18. Sun, C.; Zhang, F.; Wang, X.; Cheng, F. Facile preparation of ammonium molybdophosphate/Al-MCM-41 composite material from natural clay and its use in cesium ion adsorption. *Eur. J. Inorg. Chem.* **2015**, *2015*, 2125–2131. [CrossRef]
19. Abdullayev, A.; Bekheet, M.F.; Hanaor, D.A.H.; Gurlo, A. Materials and applications for low-cost ceramic membranes. *Membranes* **2019**, *9*, 105. [CrossRef] [PubMed]
20. Rashad, M.; Logesh, G.; Sabu, U.; Balasubramanian, M. A novel monolithic mullite microfiltration membrane for oil-in-water emulsion separation. *J. Membr. Sci.* **2021**, *620*, 118857. [CrossRef]
21. Elgamouz, A.; Tijani, N. From a naturally occurring-clay mineral to the production of porous ceramic membranes. *Microporous Mesoporous Mater.* **2018**, *271*, 52–58. [CrossRef]
22. Abubakar, M.; Tamin, M.N.; Saleh, M.A.; Uday, M.B.; Ahmad, N. Preparation and characterization of a nigerian mesoporous clay-based membrane for uranium removal from underground water. *Ceram. Int.* **2016**, *42*, 8212–8220. [CrossRef]
23. Yi, H.; Ai, Z.; Zhao, Y.; Zhang, X.; Song, S. Design of 3D-network montmorillonite nanosheet/stearic acid shape-stabilized phase change materials for solar energy storage. *Sol. Energy Mater. Sol. Cells* **2020**, *204*, 110233. [CrossRef]
24. Chen, C.; Ma, Y.; Wang, C. Investigation of electrochemical performance of montmorillonite clay as Li-ion battery electrode. *Sustain. Mater. Technol.* **2019**, *19*, e00086. [CrossRef]
25. Rajapakse, R.M.G.; Murakami, K.; Bandara, H.M.M.; Rajapakse, R.M.M.Y.; Velauthamurti, K.; Wijeratne, S. Preparation and characterization of electronically conducting polypyrrole-montmorillonite nanocomposite and its potential application as a cathode material for oxygen reduction. *Electrochim. Acta* **2010**, *55*, 2490–2497. [CrossRef]
26. Kim, M.H.; Cho, C.H.; Kim, J.S.; Nam, T.U.; Kim, W.-S.; Lee, T.I.; Oh, J.Y. Thermoelectric energy harvesting electronic skin (e-skin) Patch with reconfigurable carbon nanotube clays. *Nano Energy* **2021**, *87*, 106156. [CrossRef]
27. Vaia, R.A.; Price, G.; Ruth, P.N.; Nguyen, H.T.; Lichtenhan, J. Polymer/layered silicate nanocomposites as high performance ablative materials. *Appl. Clay Sci.* **1999**, *15*, 67–92. [CrossRef]
28. Atyia, M.N.; Mahdy, M.G.; Elrahman, M.A. Production and properties of lightweight concrete incorporating lightweight concrete incorporating recycled waste crushed clay bricks. *Constr. Build. Mater.* **2021**, *304*, 124655. [CrossRef]
29. Hassan, A.; Mourad, A.-H.I.; Rashid, Y.; Ismail, N.; Laghari, M.S. Thermal and structural performance of geopolymer concrete containing phase change material encapsulated in expanded clay. *Energy Build.* **2019**, *191*, 72–81. [CrossRef]
30. Madyan, O.A.; Fan, M.; Feo, L.; Hui, D. Physical properties of clay aerogel composites: An overview. *Compos. Part B Eng.* **2016**, *102*, 29–37. [CrossRef]
31. Di Credico, B.; Cobani, E.; Callone, E.; Conzatti, L.; Cristofori, D.; D'Arienzo, M.; Dirè, S.; Giannini, L.; Hanel, T.; Scotti, R.; et al. Size-controlled self-assembly of anisotropic sepiolite fibers in rubber nanocomposites. *Appl. Clay Sci.* **2018**, *152*, 51–64. [CrossRef]
32. Wang, L.; Wang, F.; Huang, B.; Tang, Q. Recent advances in superhydrophobic composites based on clay minerals. *Appl. Clay Sci.* **2020**, *198*, 105793. [CrossRef]
33. Serge, E.J.; Alla, J.P.; Belibi, P.D.B.; Mbadcam, K.J.; Fathima, N.N. Clay/polymer nanocomposites as filler materials for leather. *J. Clean. Prod.* **2019**, *237*, 117837. [CrossRef]
34. Qian, Z.; Hu, G.; Zhang, S.; Yang, M. Preparation and characterization of montmorillonite-silica nanocomposites: A sol-gel approach to modifying clay surfaces. *Phys. B Condens. Matter* **2008**, *403*, 3231–3238. [CrossRef]
35. Meera, K.M.S.; Sankar, R.M.; Murali, A.; Jainsankar, S.N.; Mandal, A.B. Sol-gel network silica/modified montmorillonite clay hybrid nanocomposites for hydrophobic surface coatings. *Colloids Surf. B Biointerfaces* **2012**, *90*, 204–210. [CrossRef] [PubMed]
36. Revelo, C.F.; Colorado, H.A. 3D printing of kaolinite clay ceramics using the Direct Ink Writing (DIW) technique. *Ceram. Int.* **2018**, *44*, 5673–5682. [CrossRef]
37. Chan, S.S.L.; Pennings, R.M.; Edwards, L.; Franks, G.V. 3D printing of clay for decorative architectural applications: Effect of solids volume fraction on rheology and printability. *Addit. Manuf.* **2020**, *35*, 101335. [CrossRef]
38. Njindam, O.R.; Njoya, D.; Mache, J.R.; Mouafon, M.; Messan, A.; Njopwouo, D. Effect of glass powder on the technological properties and microstructure of clay mixture for porcelain stoneware tiles manufacture. *Constr. Build. Mater.* **2018**, *170*, 512–519. [CrossRef]
39. Mahmoudi, S.; Srasra, E.; Zargouni, F. The use of Tunisian Barremian clay in the traditional ceramic industry: Optimization of ceramic properties. *Appl. Clay Sci.* **2008**, *42*, 125–129. [CrossRef]
40. Freyburg, S.; Schwarz, A. Influence of the clay type on the pore structure of structural ceramics. *J. Eur. Ceram. Soc.* **2007**, *27*, 1727–1733. [CrossRef]
41. Randviir, E.P.; Brownson, D.A.C.; Banks, C.E. A decade of graphene research: Production, applications and outlook. *Mater. Today* **2014**, *17*, 426–432. [CrossRef]
42. Santalucia, R.; Vacca, T.; Cesano, F.; Martra, G.; Pellegrino, F.; Scarano, D. Few-layered MoS_2 nanoparticles covering anatase TiO_2 nanosheets: Comparison between ex situ and in situ synthesis approaches. *Appl. Sci.* **2021**, *11*, 143. [CrossRef]
43. Rocha Barreto, I.A.; da Costa, M.L. Viability of Belterra clay, a widespread bauxite cover in the Amazon, as a low-cost raw material for the production of red ceramics. *Appl. Clay Sci.* **2018**, *162*, 252–260. [CrossRef]
44. Lopez-Galindo, A.; Viseras, C.; Cerezo, P. Compositional, technical and safety specifications of clays to be used as pharmaceutical and cosmetic products. *Appl. Clay Sci.* **2007**, *36*, 51–63. [CrossRef]

45. Lonzano-Morales, V.; Gardi, I.; Nir, S.; Undabeytia, T. Removal of pharmaceuticals from water by clay-cationic starch sorbents. *J. Clean. Prod.* **2018**, *190*, 703–711. [CrossRef]
46. Moussi, B.; Hajjaji, W.; Hachani, M.; Hatira, N.; Labrincha, J.A.; Yans, J.; Jamoussi, F. Numidian clay deposits as raw material for ceramics tile manufacturing. *J. Afr. Earth Sci.* **2020**, *164*, 103775. [CrossRef]
47. Gast, J.; Gundolf, K.; Cesinger, B. Doing business in a green way: A systematic review of the ecological sustainability entrepreneurship literature and future research directions. *J. Clean. Prod.* **2017**, *147*, 44–56. [CrossRef]
48. D'Amato, D.; Droste, N.; Allen, B.; Kettunen, M.; Lahtinen, K.; Korhonen, J.; Leskinen, P.; Matthies, B.D.; Toppinen, A. Green, circular, bio economy: A comparative analysis of sustainability avenues. *J. Clean. Prod.* **2017**, *168*, 716–734. [CrossRef]
49. Mies, A.; Gold, S. Mapping the social dimension of the circular economy. *J. Clean. Prod.* **2021**, *321*, 128960. [CrossRef]
50. Chemat, F.; Vian, M.A.; Ravi, H.K. Toward petroleum-free with plant-based chemistry. *Curr. Opin. Green Sustain. Chem.* **2021**, *28*, 100450. [CrossRef]
51. Gholizadeh, M.; Hu, X.; Liu, Q. A mini review of the specialties of the bio-oils produced from pyrolysis of 20 different biomasses. *Renew. Sustain. Energy Rev.* **2019**, *114*, 109313. [CrossRef]
52. Aziz, M.; Darmawan, A.; Juangsa, F.B. Hydrogen production from biomasses and wastes: A technological review. *Int. J. Hydrog. Energy* **2021**, *46*, 33756–33781. [CrossRef]
53. Tabasso, S.; Ginepro, M.; Tomasso, L.; Montoneri, E.; Nisticò, R.; Francavilla, M. Integrated biochemical and chemical processing of municipal bio-waste to obtain bio based products for multiple uses. The case of soil remediation. *J. Clean. Prod.* **2020**, *245*, 119191. [CrossRef]
54. Kerton, F.M.; Liu, Y.; Omari, K.W.; Hawboldt, K. Green chemistry and the ocean-based biorefinery. *Green Chem.* **2013**, *15*, 860–871. [CrossRef]
55. Zhou, Y.; Qin, S.; Verma, S.; Sar, T.; Sarsaiya, S.; Ravindran, B.; Liu, T.; Sindhu, R.; Patel, A.K.; Binod, P.; et al. Production and beneficial impact of biochar for environmental application: A comprehensive review. *Bioresour. Technol.* **2021**, *337*, 125451. [CrossRef]
56. Feng, Q.; Wang, B.; Chen, M.; Wu, P.; Lee, X.; Xing, Y. Invasive plants as potential sustainable feedstock for biochar production and multiple applications: A review. *Resour. Conserv. Recycl.* **2021**, *164*, 105204. [CrossRef]
57. Qiu, M.; Sun, K.; Jin, J.; Gao, B.; Yan, Y.; Han, L.; Wu, F.; Xing, B. Properties of the plant- and manure-derived biochars and their sorption of dibutyl phthalate and phenanthrene. *Sci. Rep.* **2014**, *4*, 5295. [CrossRef]
58. Anceschi, A.; Guerretta, F.; Magnacca, G.; Zanetti, M.; Benzi, P.; Trotta, F.; Caldera, F.; Nisticò, R. Sustainable N-containing biochars obtained at low temperatures as sorbing materials for environmental application: Municipal biowaste-derived substances and nanosponges case studies. *J. Anal. Appl. Pyrolysis* **2018**, *134*, 606–613. [CrossRef]
59. Nisticò, R.; Guerretta, F.; Benzi, P.; Magnacca, G. Chitosan-derived biochars obtained at low pyrolysis temperatures for potential application in electrochemical energy storage devices. *Int. J. Biol. Macromol.* **2020**, *164*, 1825–1831. [CrossRef]
60. Abbasi, A.; Pishvaee, M.S.; Mohseni, S. Third-generation biofuel supply chain: A comprehensive review and future research directions. *J. Clean. Prod.* **2021**, *323*, 129100. [CrossRef]
61. Molino, A.; Larocca, V.; Chianese, S.; Musmarra, D. Biofuels production by biomass gasification: A review. *Energies* **2018**, *11*, 811. [CrossRef]
62. Observatory of Economic Complexity (OEC), Which Countries Exports Clays? Available online: https://oec.world/en/visualize/tree_map/hs92/export/show/all/52508/2019/ (accessed on 10 October 2021).
63. Observatory of Economic Complexity (OEC), Which Countries Imports Clays? Available online: https://oec.world/en/visualize/tree_map/hs92/import/show/all/52508/2019/ (accessed on 10 October 2021).
64. Martin, R.T.; Bailey, S.W.; Eberl, D.D.; Fanning, D.S.; Guggenheim, S.; Kodama, H.; Pevear, D.R.; Środoń, J.; Wicks, F.J. Report of the Clay Minerals Society Nomenclature Committee: Revised classification of clay materials. *Clays Clay Miner.* **1991**, *39*, 333–335. [CrossRef]
65. Salles, F.; Henry, M.; Douilland, J.-M. Determination of the surface energy of kaolinite and serpentine using PACHA formalism—Comparison with immersion experiments. *J. Colloid Interface Sci.* **2006**, *303*, 617–626. [CrossRef]
66. Zhang, J.; Hu, L.; Pant, R.; Yu, Y.; Wei, Z.; Zhang, G. Effects of interlayer interactions on the nanoindentation behavior and hardness of 2:1 phyllosilicates. *Appl. Clay Sci.* **2013**, *80–81*, 267–280. [CrossRef]
67. Bailey, L.; Lekkerkerker, H.N.W.; Maitland, G.C. Smectite clay–inorganic nanoparticle mixed suspensions: Phase behaviour and rheology. *Soft Matter* **2015**, *11*, 222–236. [CrossRef]
68. Rashad, A.M. Vermiculite as a construction material—A short guide for civil engineer. *Constr. Build. Mater.* **2016**, *125*, 53–62. [CrossRef]
69. De Poel, W.; Vaessen, S.L.; Drnec, J.; Engwerda, A.H.J.; Townsend, E.R.; Pintea, S.; de Jong, A.E.F.; Jankowski, M.; Carlà, F.; Felici, R.; et al. Metal ion-exchange on the muscovite mica surface. *Surf. Sci.* **2017**, *665*, 56–61. [CrossRef]
70. Cao, Z.; Liu, G.; Meng, W.; Wang, P.; Yang, C. Origin of different chlorite occurrences and their effects on tight clastic reservoir porosity. *J. Pet. Sci. Eng.* **2018**, *160*, 384–392. [CrossRef]
71. Damasceno Junior, E.; Ferreira de Almeida, J.M.; do Nascimiento Silva, I.; Moreira de Assis, M.L.; dos Santos, L.M.; Dias, E.F.; Bezerra Aragao, V.E.; Verissimo, L.M.; Fernandes, N.S.; de Silva, D.R. pH-responsive release system of isoniazid using palygorskite as a nanocarrier. *J. Drug Deliv. Sci. Technol.* **2020**, *55*, 101399. [CrossRef]

72. Garcia-Rivas, J.; Sanchez del Rio, M.; Garcia-Romero, E.; Suarez, M. An insight in the structure of a palygorskite from Palygorskaja: Some questions on the standard model. *Appl. Clay Sci.* **2017**, *148*, 39–47. [CrossRef]
73. Esteban-Cubillo, A.; Pina-Zapardiel, R.; Moya, J.S.; Barba, M.F.; Pecharroman, C. The role of magnesium on the stability of crystalline sepiolite structure. *J. Eur. Ceram. Soc.* **2008**, *28*, 1763–1768. [CrossRef]
74. Hong, H.; Churchman, G.J.; Gu, Y.; Yin, K.; Wang, C. Kaolinite-smectite mixed-layer clays in the Jiujiang red soils and their climate significance. *Geoderma* **2012**, *173–174*, 75–83. [CrossRef]
75. Van Ranst, E.; Kips, P.; Mbogoni, J.; Mees, F.; Dumon, M.; Delvaux, B. Halloysite-smectite mixed-layered clay in fluvio-volcanic soils at the southern foot of Mount Kilimanjaro, Tanzania. *Geoderma* **2020**, *375*, 114527. [CrossRef]
76. Kumari, N.; Mohan., C. Basics of Clay Minerals and Their Characteristic Properties. In *Clay and Clay Minerals*; Morari Do Nascimento, G., Ed.; IntechOpen: London, UK, 2021. Available online: https://www.intechopen.com/online-first/76780 (accessed on 10 October 2021). [CrossRef]
77. Thakur, A.; Jaiswal, M.K.; Peak, C.W.; Carrow, J.K.; Gentry, J.; Dolatshahi-Pirouz, A.; Gaharwar, A.K. Injectable shear thinning nanoengineered hydrogels for stem cell delivery. *Nanoscale* **2016**, *8*, 12362–12372. [CrossRef] [PubMed]
78. Kerativitayanan, P.; Tatullo, M.; Khariton, M.; Joshi, P.; Perniconi, B.; Gaharwar, A.K. Nanoengineered osteoinductive and elastomeric scaffolds for bone tissue enginnering. *ACS Biomater. Sci. Eng.* **2017**, *3*, 590–600. [CrossRef]
79. Schiffman, J.D.; Schauer, C.L. A review: Electrospinning of biopolymer nanofibers and their applications. *Polym. Rev.* **2008**, *48*, 317–352. [CrossRef]
80. Hong, J.-H.; Jeong, E.H.; Lee, H.S.; Baik, D.H.; Seo, S.W.; Youk, J.H. Electrospinning of polyurethane/organically modified montmorillonite nanocomposites. *J. Polym. Sci. Part B Polym. Phys.* **2005**, *43*, 3171–3177. [CrossRef]
81. Gungor-Ozkerim, P.S.; Inci, I.; Zhang, Y.S.; Khademhosseini, A.; Dokmeci, M.R. Bioinks for 3D bioprinting: An overview. *Biomater. Sci.* **2018**, *6*, 915–946. [CrossRef] [PubMed]
82. DeSimone, E.; Schacht, K.; Pellert, A.; Scheibel, T. Recombinant spider silk-based bioinks. *Biofabrication* **2017**, *9*, 044104. [CrossRef] [PubMed]
83. Kang, H.-W.; Lee, S.J.; Ko, I.K.; Kengla, C.; Yoo, J.J.; Atala, A. A 3D bioprinting system to produce human-scale tissue constructs with structural integrity. *Nat. Biotechnol.* **2016**, *34*, 312–319. [CrossRef]
84. El-Husseiny, H.M.; Mady, E.A.; Hamabe, L.; Abugomaa, A.; Shimada, K.; Yoshida, T.; Tanaka, T.; Yokoi, A.; Elbadawy, M.; Tanaka, R. Smart/stimuli-responsive hydrogels: Cutting edge platforms for tissue engineering and other biomedical applications. *Mater. Today Bio* **2022**, *13*, 100186. [CrossRef] [PubMed]
85. Unagolla, J.M.; Jayasuriya, A.C. Hydrogel-based 3D bioprinting: A comprehensive review on cell-laden hydrogels, bioink formulations and future perspectives. *Appl. Mater. Today* **2020**, *18*, 100479. [CrossRef] [PubMed]
86. Guo, J.; Zhang, R.; Zhang, L.; Cao, X. 4D printing of robust hydrogels consisted of agarose nanofibers and polyacrylamide. *ACS Macro Lett.* **2018**, *7*, 442–446. [CrossRef]
87. Lazzara, G.; Cavallaro, G.; Panchal, A.; Fakhrullin, R.; Stavitskaya, A.; Vinokurov, V.; Lvov, Y. An assembly of organic-inorganic composites using halloysite clay nanotube. *Curr. Opin. Colloid Interface Sci.* **2018**, *35*, 42–50. [CrossRef]
88. Cervini-Silva, J.; Ramirez-Apan, M.T.; Kaufhold, S.; Ufer, K.; Palacios, E.; Montoya, A. Role of bentonite clays on cell growth. *Chemosphere* **2016**, *149*, 57–61. [CrossRef] [PubMed]
89. Abduljauwad, S.N.; Ahmed, H.-u.-R.; Moy, V.T. Melanoma treatment via non-specific adhesion of cancer cells using charged nano-clays in pre-clinical studies. *Sci. Rep.* **2021**, *11*, 2737. [CrossRef] [PubMed]
90. Lin, F.H.; Lee, Y.H.; Jian, C.H.; Wong, J.-M.; Shieh, M.-J.; Wang, C.-Y. A study of purified montmorillonite intercalated with 5-fluorouracil as drug carrier. *Biomaterials* **2002**, *9*, 1981–1987. [CrossRef]
91. Yu, M.; Pan, L.; Sun, L.; Li, J.; Shang, J.; Zhang, S.; Liu, D.; Li, W. Supramolecular assemblies constructed from β-cyclodextrin-modified montmorillonite nanosheets as carrier for 5-fluorouracil. *J. Mater. Chem. B* **2015**, *3*, 9043–9052. [CrossRef]
92. Tabasi, H.; Oroojalian, F.; Darroudi, M. Green clay ceramics as potential nanovehicles for drug delivery applications. *Ceram. Int.* **2021**, *47*, 31042–31053. [CrossRef]
93. Zhu, T.; Ma, X.; Chen, R.; Ge, Z.; Xu, J.; Shen, X.; Jia, L.; Zhou, T.; Luo, Y.; Ma, T. Using fluorescently-labeled magnetic nanocomposites as a dual contrast agent for optical and magnetic resonance imaging. *Biomater. Sci.* **2017**, *5*, 1090–1100. [CrossRef] [PubMed]
94. Gianni, E.; Avgoustakis, K.; Papoulis, D. Kaolinite group minerals: Applications in cancer diagnosis and treatment. *Eur. J. Pharm. Biopharm.* **2020**, *154*, 359–376. [CrossRef] [PubMed]
95. Nisticò, R.; Cesano, F.; Garello, F. Magnetic materials and systems: Domain structure visualization and other characterization techniques for the application in the materials science and biomedicine. *Inorganics* **2020**, *8*, 6. [CrossRef]
96. Jury, W.A.; Vaux Jr., H. The role of science in solving the world's emerging water problems. *Proc. Natl. Acad. Sci. USA* **2005**, *102*, 15715–15720. [CrossRef]
97. Maier, J.; Palazzo, J.; Geyer, R.; Steigerwald, D.G. How much potable water is saved by wastewater recycling? Quasi-experimental evidence from California. *Resour. Conserv. Recycl.* **2022**, *176*, 105948. [CrossRef]
98. Jain, M.; Khan, S.A.; Sharma, K.; Jadhao, P.R.; Pant, K.K.; Ziora, Z.M.; Blaskovich, M.A.T. Current perspective of innovative strategies for bioremediation of organic pollutants from wastewater. *Bioresour. Technol.* **2022**, *344*, 126305. [CrossRef] [PubMed]
99. Jain, M.; Khan, S.A.; Pandey, A.; Pant, K.K.; Ziora, Z.M.; Blaskovich, M.A.T. Instructive analysis of engineered carbon materials for potential application in water and wastewater treatment. *Sci. Total Environ.* **2021**, *793*, 148583. [CrossRef] [PubMed]

100. Jaspal, D.; Malviya, A. Composites for wastewater purification: A review. *Chemosphere* **2020**, *246*, 125788. [CrossRef] [PubMed]
101. Rostam, A.B.; Taghizadeh, M. Advanced oxidation processes integrated by membrane reactors and bioreactors for various wastewater treatments: A critical review. *J. Environ. Chem. Eng.* **2020**, *8*, 104566. [CrossRef]
102. Polliotto, V.; Pomilla, F.R.; Maurino, V.; Marcì, G.; Bianco Prevot, A.; Nisticò, R.; Magnacca, G.; Paganini, M.C.; Ponce Robles, L.; Perez, L.; et al. Different approaches for the solar photocatalytic removal of micro-contaminants from aqueous environment: Titania vs. hybrid magnetic iron oxides. *Catal. Today* **2019**, *328*, 164–171. [CrossRef]
103. Bianco Prevot, A.; Baino, F.; Fabbri, D.; Franzoso, F.; Magnacca, G.; Nisticò, R.; Arques, A. Urban biowaste-derived sensitizing materials for caffeine photodegradation. *Environ. Sci. Pollut. Res.* **2017**, *24*, 12599–12607. [CrossRef] [PubMed]
104. Owodunni, A.A.; Ismail, S. Revolutionary technique for sustainable plant-based green coagulants in industrial wastewater treatment-A review. *J. Water Process Eng.* **2021**, *42*, 102096. [CrossRef]
105. Peralta, M.E.; Martire, D.O.; Moreno, M.S.; Parolo, M.E.; Carlos, L. Versatile nanoadsorbents based on magnetic mesostructured silica nanoparticles with tailored surface properties for organic pollutants removal. *J. Environ. Chem. Eng.* **2021**, *9*, 104841. [CrossRef]
106. Nisticò, R.; Tabasso, S.; Magnacca, G.; Jordan, T.; Shalom, M.; Fechler, N. Reactive hypersaline route: One-pot synthesis of porous photoactive nanocomposites. *Langmuir* **2017**, *33*, 5213–5222. [CrossRef] [PubMed]
107. Goh, P.S.; Wong, K.C.; Ismail, A.F. Membrane technology: A versatile tool for saline wastewater treatment and resource recovery. *Desalination* **2022**, *521*, 115377. [CrossRef]
108. Asif, M.B.; Zhang, Z. Ceramic membrane technology for water and wastewater treatment: A critical review of performance, full-scale applications, membrane fouling and prospects. *Chem. Eng. J.* **2021**, *418*, 129481. [CrossRef]
109. Lofrano, G.; Brown, J. Wastewater management through the ages: A history of mankind. *Sci. Total Environ.* **2010**, *408*, 5254–5264. [CrossRef] [PubMed]
110. Plazinski, W.; Rudzinski, W.; Plazinska, A. Theoretical models of sorption kinetics including a surface reaction mechanism: A review. *Adv. Colloid Interface Sci.* **2009**, *152*, 2–13. [CrossRef]
111. Bentahar, Y.; Hurel, C.; Draoui, K.; Khairoun, S.; Marmier, N. Adsorptive properties of Maroccan clays for the removal of arsenic(V) from aqueous solution. *Appl. Clay Sci.* **2016**, *119*, 385–392. [CrossRef]
112. Veli, S.; Alyuz, B. Adsorption of copper and zinc from aqueous solutions by using natural clay. *J. Hazard. Mater.* **2007**, *149*, 226–233. [CrossRef] [PubMed]
113. Bhattacharyya, K.G.; Gupta, S.S. Adsorption of chromium(VI) from water by clays. *Ind. Eng. Chem. Res.* **2006**, *45*, 7232–7240. [CrossRef]
114. Farrah, H.; Pickering, W.F. pH effects in the adsorption of heavy metal ions by clays. *Chem. Geol.* **1979**, *25*, 317–326. [CrossRef]
115. Priyantha, N.; Bandaranayaka, A. Interaction of Cr(VI) species with thermally treated brick clay. *Environ. Sci. Pollut. Res.* **2011**, *18*, 75–81. [CrossRef]
116. Chen, L.; Zhou, C.H.; Fiore, S.; Tong, D.S.; Zhang, H.; Li, C.S.; Ji, S.F.; Yu, W.H. Functional magnetic nanoparticle/clay mineral nanocomposites: Preparation, magnetism and versatile applications. *Appl. Clay Sci.* **2016**, *127–128*, 143–163. [CrossRef]
117. Leonel, A.G.; Mansur, A.A.P.; Mansur, H.S. Advanced functional nanostructures based on magnetic iron oxide nanomaterials for water remediation: A review. *Water Res.* **2021**, *190*, 116693. [CrossRef]
118. Panda, S.K.; Aggarwal, I.; Kumar, H.; Prased, L.; Kumar, A.; Sharma, A.; Vo, D.-V.N.; Thuan, D.V.; Mishra, V. Magnetite nanoparticles as sorbents for dye removal: A review. *Environ. Chem. Lett.* **2021**, *19*, 2487–2525. [CrossRef]
119. Nisticò, R. Magnetic materials and water treatments for a sustainable future. *Res. Chem. Intermed.* **2017**, *43*, 6911–6949. [CrossRef]
120. Najafi, H.; Farajfaed, S.; Zolgharnian, S.; Mirak, S.H.M.; Asasian-Kolur, N.; Sharifian, S. A comprehensive study in modified-pillared clays as ad adsorbent in wastewater treatment processes. *Process Saf. Environ. Prot.* **2021**, *147*, 8–36. [CrossRef]
121. Nisticò, R. A synthetic guide toward the tailored production of magnetic iron oxide nanoparticles. *Bol. Soc. Esp. Cerám. V.* **2021**, *60*, 29–40. [CrossRef]
122. Chiu, C.-W.; Huang, T.-K.; Wang, Y.-C.; Alamani, B.G.; Lin, J.-J. Intercalation strategies in clay/polymer hybrids. *Prog. Polym. Sci.* **2014**, *39*, 443–485. [CrossRef]
123. Magdy, A.; Fouad, Y.O.; Abdel-Aziz, M.H.; Konsowa, A.H. Synthesis and characterization of Fe_3O_4/kaolin magnetic nanocomposite and its application in wastewater treatment. *J. Ind. Eng. Chem.* **2017**, *56*, 299–311. [CrossRef]
124. Coha, M.; Farinelli, G.; Tiraferri, A.; Minella, M.; Vione, D. Advanced oxidation processes in the removal of organic substances form produced water: Potential, configurations, and research needs. *Chem. Eng. J.* **2021**, *414*, 128668. [CrossRef]
125. Brillas, E. A review on the photoelectro-Fenton process as efficient electrochemical advanced oxidation for wastewater remediation. Treatment with UV light, sunlight, and coupling with conventional and other photo-assisted advanced technologies. *Chemosphere* **2020**, *250*, 126198. [CrossRef] [PubMed]
126. Mansouri, L.; Tizaoui, C.; Geissen, S.-U.; Bousselmi, L. A comparative study on ozone, hydrogen peroxide and UV based advanced oxidation processes for efficient removal of diethyl phthalate in water. *J. Hazard. Mater.* **2019**, *363*, 401–411. [CrossRef] [PubMed]
127. Rekhate, C.V.; Srivastava, J.K. Recent advances in ozone-based advanced oxidation processes for treatment of wastewater—A review. *Chem. Eng. J. Adv.* **2020**, *3*, 100031. [CrossRef]
128. Kurian, M. Advanced oxidation processes and nanomaterials—A review. *Clean. Eng. Technol.* **2021**, *2*, 100090. [CrossRef]

129. Andreozzi, R.; Caprio, V.; Insola, A.; Marotta, R. Advanced oxidation processes (AOP) for water purification and recovery. *Catal. Today* **1999**, *53*, 51–59. [CrossRef]
130. Sanakousar, F.M.; Vidyasagar, C.C.; Jimenez-Perez, V.M.; Prakash, K. Recent progress on visible-light-driven metal and non-metal doped ZnO nanostructures for photocatalytic degradation of organic pollutants. *Mater. Sci. Semicond. Process.* **2022**, *140*, 106390. [CrossRef]
131. Bianco Prevot, A.; Arques, A.; Carlos, L.; Laurenti, E.; Magnacca, G.; Nisticò, R. Innovative sustainable materials for the photoinduced remediation of polluted water. In *Sustainable Water and Wastewater Processes*; Galanakis, C.M., Agrafioti, E., Eds.; Elsevier Inc.: Amsterdam, The Netherlands, 2019; Chapter 7; pp. 203–238, ISBN 978-0-12-816170-8. [CrossRef]
132. Singh, P.; Sharma, K.; Hasija, V.; Sharma, V.; Sharma, S.; Raizada, P.; Singh, M.; Saini, A.K.; Hosseini-Bandegharaei, A.; Thakur, V.K. Systematic review on applicability of magnetic iron oxides-integrated photocatalysts for degradation of organic pollutants in water. *Mater. Today Chem.* **2019**, *14*, 100186. [CrossRef]
133. Azzam, M.O.J. Olive mills wastewater treatment using mixed adsorbents of volcanic tuff, natural clay and charcoal. *J. Environ. Chem. Eng.* **2018**, *6*, 2126–2136. [CrossRef]
134. De Paiva, L.B.; Morales, A.R.; Valenzuela Diaz, F.R. Organoclays: Properties, preparation and applications. *Appl. Clay Sci.* **2008**, *42*, 8–24. [CrossRef]
135. Vaia, R.A.; Teukolsky, R.K.; Giannelis, E.P. Interlayer structure and molecular environment of alkylammonium layered silicates. *Chem. Mater.* **1994**, *6*, 1017–1022. [CrossRef]
136. Foorginezhad, S.; Zerafat, M.M. Microfiltration of cationic dyes using nano-clay membranes. *Ceram. Int.* **2017**, *43*, 15146–15159. [CrossRef]
137. Blyweert, P.; Nicolas, V.; Fierro, V.; Celzard, A. 3D printing of carbon-based materials: A review. *Carbon* **2021**, *183*, 449–485. [CrossRef]
138. Ngo, T.D.; Kashani, A.; Imbalzano, G.; Nguyen, K.T.Q.; Hui, D. Additive manufacturing (3D printing): A review of materials, methods, applications and challenges. *Compos. Part B Eng.* **2018**, *143*, 172–196. [CrossRef]
139. Singh, T.; Kumar, S.; Sehgal, S. 3D printing of engineering materials: A state of the art review. *Mater. Today Proc.* **2020**, *28*, 1927–1931. [CrossRef]
140. Zhang, B.; Goel, A.; Ghalsasi, O.; Anand, S. CAD-based design and pre-processing tools for additive manufacturing. *J. Manuf. Syst.* **2019**, *52*, 227–241. [CrossRef]
141. Cano-Vicent, A.; Tambuwala, M.M.; Hassan, S.S.; Barh, D.; Aljabali, A.A.A.; Birkett, M.; Arjunan, A.; Serrano-Aroca, A. Fused deposition modelling: Current status, methodology, applications and future prospects. *Addit. Manuf.* **2021**, *47*, 102378. [CrossRef]
142. Anand, M.; Das, A.K. Issues in fabrication of 3D components through DMLS Technique: A review. *Opt. Laser Technol.* **2021**, *139*, 106914. [CrossRef]
143. Nouri, A.; Shirvan, A.R.; Li, Y.; Wen, C. Additive manufacturing of metallic and polymeric load-bearing biomaterials using laser powder bed fusion: A review. *J. Mater. Sci. Technol.* **2021**, *94*, 196–215. [CrossRef]
144. Dowling, L.; Kennedy, J.; O'Shaughnessy, S.; Trimble, D. A review of critical repeatability and reproducibility issues in powder bed fusion. *Mater. Des.* **2020**, *186*, 108346. [CrossRef]
145. Aboulkhair, N.T.; Simonelli, M.; Perry, L.; Ashcroft, I.; Tuck, C.; Hague, R. 3D printing of aluminium alloys: Additive manufacturing of aluminium alloys using selective laser melting. *Prog. Mater. Sci.* **2019**, *106*, 100578. [CrossRef]
146. Gonzalez-Henriquez, C.M.; Sarabia-Vallejos, M.A.; Rodriguez-Hernandez, J. Polymers for additive manufacturing and 4D-printing: Materials, methodologies, and biomedical applications. *Prog. Polym. Sci.* **2019**, *94*, 57–116. [CrossRef]
147. Chen, Z.; Li, Z.; Li, J.; Liu, C.; Lao, C.; Fu, Y.; Liu, C.; Li, Y.; Wang, P.; He, Y. 3D printing of ceramics: A review. *J. Eur. Ceram. Soc.* **2019**, *39*, 661–687. [CrossRef]
148. Mustapha, K.B.; Metwalli, K.M. A review of fused deposition modelling for 3D printing of smart polymeric materials and composites. *Eur. Polym. J.* **2021**, *156*, 110591. [CrossRef]
149. Xiao, J.; Ji, G.; Zhang, Y.; Ma, G.; Mechtcherine, V.; Pan, J.; Wang, L.; Ding, T.; Duan, Z.; Du, S. Large-scale 3D printing concrete technology: Current status and future opportunities. *Cem. Concr. Compos.* **2021**, *122*, 104115. [CrossRef]
150. Rajabi, M.; McConnell, M.; Cabral, J.; Ali, M.A. Chitosan hydrogels in 3D printing for biomedical applications. *Carbohydr. Polym.* **2021**, *260*, 117768. [CrossRef]
151. Oladapo, B.I.; Zahedi, S.A.; Ismail, S.O.; Omigbodun, F.T. 3D printing of PEEK and its composite to increase biointerfaces as a biomedical material—A review. *Colloids Surf. B Biointerfaces* **2021**, *203*, 111726. [CrossRef]
152. Gao, C.; Lu, C.; Jian, Z.; Zhang, T.; Chen, Z.; Zhu, Q.; Tai, Z.; Liu, Y. 3D bioprinting for fabricating artificial skin tissue. *Colloids Surf. B Biointerfaces* **2021**, *208*, 112041. [CrossRef]
153. Hann, S.Y.; Cui, H.; Esworthy, T.; Miao, S.; Zhou, X.; Lee, S.-J.; Fisher, J.P.; Zhang, L.G. Recent advances in 3D printing: Vascular network for tissue and organ regeneration. *Transl. Res.* **2019**, *211*, 46–63. [CrossRef]
154. Wilms, P.; Daffner, K.; Kern, C.; Gras, S.L.; Schutyser, M.A.I.; Kohlus, R. Formulation engineering of food systems for 3D-printing applications—A review. *Food Res. Int.* **2021**, *148*, 110585. [CrossRef]
155. Chen, Y.; He, S.; Zhang, Y.; Wan, Z.; Copuroglu, O.; Schlangen, E. 3D printing of calcined clay-limestone-based cementitious materials. *Cem. Concr. Res.* **2021**, *149*, 106553. [CrossRef]
156. Long, W.-J.; Lin, C.; Tao, J.L.; Ye, T.-H.; Fang, Y. Printability and particle packing of 3D-printable limestone calcined clay cement composites. *Constr. Build. Mater.* **2021**, *282*, 122647. [CrossRef]

157. Faksawat, K.; Limsuwan, P.; Naemchanthara, K. 3D printing technique of specific bone shape based on raw clay using hydroxyapatite as an additive material. *Appl. Clay Sci.* **2021**, *214*, 106269. [CrossRef]
158. Chikkangoudar, R.N.; Sachidananda, T.G.; Pattar, N. Influence of 3D printing parameters on the dimensional stability of polypropylene/clay printed parts using laser scanning technique. *Mater. Today Proc.* **2021**, *44*, 4118–4123. [CrossRef]
159. Brinker, C.J.; Scherer, G.W. *Sol-Gel Science: The Physics and Chemistry of Sol-Gel Processing*; Academic Press: San Diego, CA, USA, 1990; ISBN 9780080571034.
160. Hench, L.L.; West, J.K. The sol-gel process. *Chem. Rev.* **1990**, *90*, 33–72. [CrossRef]
161. Nisticò, R.; Scalarone, D.; Magnacca, G. Sol-gel chemistry, templating and spin-coating deposition: A combined approach to control in a simple way the porosity of inorganic thin films/coatings. *Microporous Mesoporous Mater.* **2017**, *248*, 18–29. [CrossRef]
162. Ciriminna, R.; Fidalgo, A.; Pandarus, V.; Beland, F.; Ilharco, L.M.; Pagliaro, M. The sol-gel route to advanced silica-based materials and recent applications. *Chem. Rev.* **2013**, *113*, 6592–6620. [CrossRef]
163. Pierre, A.C.; Pajonk, G.M. Chemistry of aerogels and their applications. *Chem. Rev.* **2002**, *102*, 4243–4266. [CrossRef]
164. Lofgreen, J.E.; Ozin, G.A. Controlling morphology and porosity to improve performance of molecularly imprinted sol-gel silica. *Chem. Soc. Rev.* **2014**, *43*, 911–933. [CrossRef]
165. Zhang, Q.; Wang, W.; Goebl, J.; Yin, Y. Self-templated synthesis of hollow nanostructures. *Nano Today* **2009**, *4*, 494–507. [CrossRef]
166. Nisticò, R.; Magnacca, G.; Antonietti, M.; Fechler, N. "Salted silica": Sol-gel chemistry of silica under hypersaline conditions. *Z. Anorg. Allg. Chem.* **2014**, *640*, 582–587. [CrossRef]
167. Pronina, N.; Klauson, D.; Moiseev, A.; Deubener, J.; Krichevskaya, M. Titanium dioxide sol-gel coated expanded clay granules for use in photocatalytic fluidized-bed reactor. *Appl. Catal. B Environ.* **2015**, *178*, 117–123. [CrossRef]